BIOMIMETICS

Exploration of underwater life with an acoustically controlled soft robotic fish

Robert K. Katzschmann,* Joseph DelPreto, Robert MacCurdy, Daniela Rus

Closeup exploration of underwater life requires new forms of interaction, using biomimetic creatures that are capable of agile swimming maneuvers, equipped with cameras, and supported by remote human operation. Current robotic prototypes do not provide adequate platforms for studying marine life in their natural habitats. This work presents the design, fabrication, control, and oceanic testing of a soft robotic fish that can swim in three dimensions to continuously record the aquatic life it is following or engaging. Using a miniaturized acoustic communication module, a diver can direct the fish by sending commands such as speed, turning angle, and dynamic vertical diving. This work builds on previous generations of robotic fish that were restricted to one plane in shallow water and lacked remote control. Experimental results gathered from tests along coral reefs in the Pacific Ocean show that the robotic fish can successfully navigate around aquatic life at depths ranging from 0 to 18 meters. Furthermore, our robotic fish exhibits a lifelike undulating tail motion enabled by a soft robotic actuator design that can potentially facilitate a more natural integration into the ocean environment. We believe that our study advances beyond what is currently achievable using traditional thruster-based and tethered autonomous underwater vehicles, demonstrating methods that can be used in the future for studying the interactions of aquatic life and ocean dynamics.

INTRODUCTION

Problem addressed

Closeup and minimally disruptive observations of marine life are particularly useful when studying animals' behaviors, swim patterns, and interactions within their habitats (*1*, *2*). A biomimetic underwater observatory for long-term studies could facilitate deeper understanding of marine life, especially their social behaviors and how environmental changes affect the delicate balance within the marine world. One possibility to achieve this is using underwater vehicles that can swim alongside marine life to allow closeup observations. Remotely operated vehicles (ROVs) or autonomous underwater vehicles (AUVs) in ocean environments typically use propellers or jet-based propulsion systems (*3*). However, these propulsion systems generate substantial turbulence and have the potential to scare marine life and to prevent closeup observations (*4*). Further, the mere appearance of these vehicles, typically large and rigid like a submarine, does not integrate well into the marine environment. The complexity of most traditional ROVs also requires costly fabrication and intricate control strategies, and their large bulk restricts their tethered deployment to deeper water using specially equipped vessels. Smaller ROVs also generally require tethers, which can be cumbersome and restrict operation.

To address this problem, we sought to create biomimetic fish robots that can be easily used by a single diver. We also wanted to generate lifelike undulation of the robotic fish tail for propulsion and to enable untethered remote control of these fish robots by a diver. Our solution is a soft underwater robot with fluid-driven actuation that swims with compliant and continuous strokes that imitate the movement of fish. Biomimicry potentially increases the ability of robots to approach marine life without disturbing them (*5*, *6*) or their natural environment. Despite the emergence of previously unknown actuation modalities (*7*) that could also enable undulatory or oscillatory biomimetic locomotion underwater (*8*, *9*), none of the benchtop robotic fish prototypes reported in literature can swim untethered in three dimensions for prolonged periods of time at a range of depths.

This paper describes our Soft Robotic Fish (SoFi), which builds on the basic design philosophy of previous robotic fish prototypes that we have constructed. In contrast to earlier efforts, this robot has onboard capabilities for untethered operation in ocean environments, including the ability to move along three-dimensional (3D) trajectories by adjusting its dive planes or by controlling its buoyancy. Onboard sensors perceive the environment, and a mission control system enables a human diver to issue remote commands. SoFi advances our previous work on soft robotic fish in several dimensions. The first-generation fish (*10*) was suspended underwater and pneumatically actuated to swim forward at a fixed depth and to execute escape maneuvers. The second-generation fish (*11*) used hydraulic soft actuation and incorporated dive planes for dynamic diving. However, the robot had limited thrust, could not withstand compression at depths of more than a meter, was not able to adjust its buoyancy autonomously, and had no mechanism for underwater remote control and communication with a human diver. This paper also builds on our acoustic communication modem documented in (*12*), presenting its integration into SoFi and evaluating its ability to enable real-time interactive oceanic exploration. SoFi integrates and extends these previous works, achieving untethered swimming and remote control at a range of depths in complex environments.

Paper's importance

SoFi is capable of close observations of marine life and has the potential to be a new platform for studying and interacting with underwater species. It demonstrates that a soft fluidic actuator can be a successful propulsive mechanism for prolonged untethered underwater exploration at multiple depths.

In particular, this work presents (i) a powerful hydraulic soft actuator, (ii) a control mechanism that allows the robot to adjust its buoyancy according to depth, (iii) onboard sensors to observe and

Distributed Robotics Laboratory, Computer Science and Artificial Intelligence Laboratory, Massachusetts Institute of Technology, Cambridge, MA 02139, USA.
*Corresponding author. Email: rkk@csail.mit.edu

record the environment, (iv) a mission control system that a human diver can use to provide navigational commands to the robot from a distance using acoustic signals, and (v) extended ocean experiments at depths ranging from 0 to 18 m. SoFi has demonstrated untethered swimming and the ability to autonomously execute high-level commands in coastal waters and coral reefs at depths of up to 18 m. In short, SoFi has the onboard capabilities of an untethered mobile underwater observatory to potentially enable nondisruptive monitoring of marine life.

Challenges in design and control

We wanted to build and successfully deploy an untethered underwater robotic fish, similar in size and behavior to living fish, that can autonomously execute high-level commands received remotely from a diver. The challenge is to realize biomimetic swimming of a self-contained system in a compact size, with good portability, limited power, and communication capabilities. The robotic fish has to execute 3D trajectories with lifelike undulatory locomotion by using a soft fluidic circulatory actuator and a compact buoyancy control mechanism. All components of the integrated end-to-end system have to be designed accordingly, including the pump, the soft actuator body, the onboard control, the energy storage, the wide-view video camera, the onboard sensors, the acoustic communication module, and the remote control interface. Two major challenges related to locomotion are (i) the creation of a hydraulic propulsion system that can carry all crucial components needed for an untethered underwater exploration and (ii) a low-drag design with appropriate buoyancy and weight distribution that can maintain structural integrity under pressure throughout a suitable depth range. To overcome these challenges and achieve biomimetic propulsion, we had to design a custom low-pressure high-flow pump and an appropriately sized soft fluidic actuator. An adjustable buoyancy unit, oil-filled chambers for electronics, custom seals, and rigid foam–filled compartments all had to fit within the limited volume available. Human interaction with the robot in the challenging underwater environment is also a design constraint. We created an underwater communication module that allows for real-time control of the robot and provides an intuitive interface in a rugged, compact, and low-power package.

Background and related work

Natural systems often exceed the performance of rigid robotic systems because of their soft and compliant characteristics, such as the unmatched speed and agility of a cheetah (13, 14) or the ability of a dead fish to swim upstream (15). The pioneering work in robotic fish was the Vorticity Control Unmanned Undersea Vehicle (16), a system using a driven link assembly to perform fish-like swimming. The hydraulic control of tuna fins (17) served as an inspiration to develop soft robotic fish with hydraulic actuation, and several reviews of soft robotic systems (18–21) have highlighted the potential advantages of deformable bodies for robotic systems. Several underwater vehicles using bioinspired locomotion mechanisms have been proposed since (8). There have been initial steps toward soft robots that mimic fish (5, 10, 11, 22, 23), mantas (24–26), lamprey (27, 28), and octopi (29, 30). Several simple fish prototypes have been proposed for studying the interaction of robotic fish with real fish in small tanks (5, 6, 31–35). None of the proposed systems have demonstrated autonomous, untethered biomimetic underwater operation in a real environment at several meters of depth (9). Furthermore, none of those systems have observed or interacted with aquatic life in their natural habitat.

There have been various design and fabrication techniques proposed for fluidic elastomer actuators. Soft lithography (36), shape deposition manufacturing (37), thread-reinforced pneumatic chambers (38), and retractable pin casting (39) were some of the initial methods that can be used to realize soft fluid actuators. None of these methods allow for the repeatable fabrication of soft fluidic actuators without weakening seams and integrated functional structures such as backbones. Three-dimensional printing of soft actuators and the creation of intelligent damping materials (40, 41) have shown that fine-grained control of various materials allows for the automated fabrication of heterogeneous structures with embedded liquids as functional actuation or passive damping channels. Although 3D printing opens previously unknown dimensions in heterogeneous actuator design, the materials available are not deformable and robust enough to undergo strong cyclical flexing. In the work presented here, we use monolithic casting using a lost-wax fabrication technique (11), a reliable and easily reproducible way to fabricate soft actuators with complex inner cavities and without seams that may compromise structural integrity.

Longevity and endurance are important challenges for self-contained soft robots. Pneumatic energy sources are commonly used for the actuation of terrestrial soft robots (42), but external pneumatic pumps constrain the mobility of a system, limiting autonomy and range. Systems using a compressed air cartridge as an onboard pressure source can only operate on the order of a few minutes because of the low-energy density of compressed air and the challenge of either recycling or venting the air after the inflation of a cavity (10). Constant release of gas causes nonnegligible changes in the overall buoyancy of the robotic fish, rendering depth control infeasible. In addition, a fixed volume of gas limits deployment time. In contrast, alternately transporting fluid from one chamber to another as carried out in SoFi does not require an extra storage unit, and the fluid does not need to be exhausted to deflate the actuator. Using water instead of air as the transmission fluid also eases deployment underwater.

There are multiple systems used to control the buoyancy of underwater robots. The major open research problem for these mechanisms is reducing weight, bulk, and noise (9). One system heats and cools wax or oil to change its buoyancy (43, 44). However, this has a slow response time, especially when cooling the medium. A second system uses a buoyancy chamber that can be filled with air or water; the water is pushed out of the chamber by filling it from a compressed air tank (45). This system is large and requires refilling of the compressed air tanks. A third system uses electrolysis to create bubbles in a 2-ml volume (46). However, as the system is scaled up in size, the realizable change in volume becomes insufficient. A fourth system, used in large underwater gliders, adjusts buoyancy by compressing or filling an air chamber and adjusts pitch by moving an internal mass (47, 48). Although these parts are reliable, the complex actuation mechanisms of the plunger or bladders are intricate, bulky, and difficult to scale down. A fifth mechanism, used in a batoid robot, also compresses air through a piston. Although smaller than the fourth system, it still has bulky external actuation parts (such as a lead screw drive) that protrude from the main body of the robot and are difficult to incorporate in other designs such as submarines or robotic fish (49). By using similar principles to this fifth mechanism but further miniaturizing the actuation, we designed a modular buoyancy system that is fast, simple, and effective in actuation and control.

Underwater communication is an essential component for AUVs. Although radio-frequency communications (50) are ubiquitous in
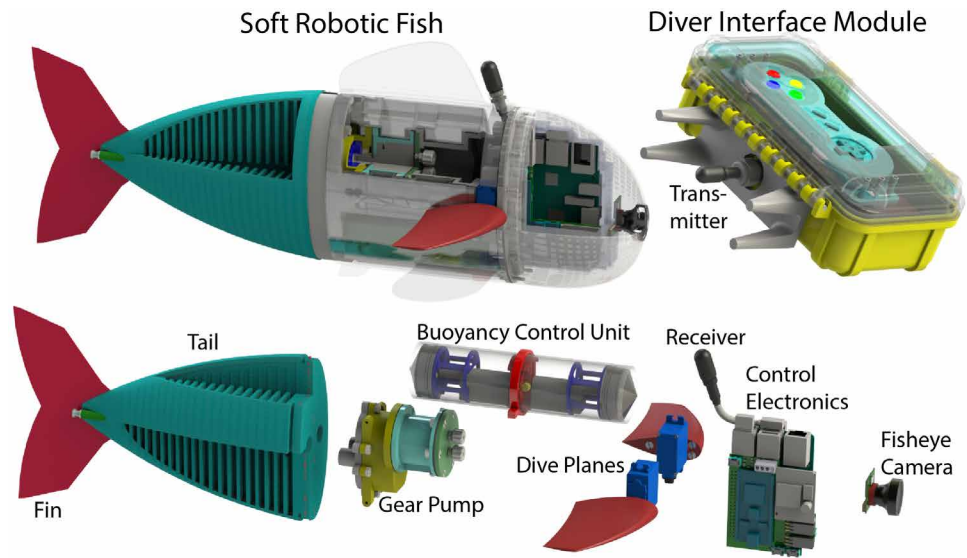
Fig. 1. SoFi system overview. (Top, left to right) Soft robotic fish and diver interface module. (**Bottom**, left to right) Subcomponents of the system are the elastomer tail (cut view), external gear pump, BCU, two dive planes, control electronics including acoustic receiver, and fisheye camera.

Fig. 2. Underwater exploration. Fish trajectory exploring a coral reef. The snapshots of the fish are equally spaced in time by 2.6 s per representation.

terrestrial applications, those signals rapidly attenuate in saltwater (*51*). Optical communications (*52–54*) are also challenging underwater because they are subject to scattering and noise from ambient light. We therefore used acoustic communications, which have been widely adopted for underwater applications (*55–57*). Although Woods Hole Oceanographic Institution modems (*58, 59*) can overcome challenges such as multipath effects and Doppler shifts (*60*), their size and power consumption are too large for fish-sized robots. Similarly, other modems (*61, 62*) focus on higher data rates and longer ranges than required for remote-controlled operation by a diver, rendering them too bulky, expensive, and energy-consuming for our present application. Some acoustic modems (*52*) use hardware-defined signal generation and detection, but this limits available processing and reduces versatility. Taking these works into account, we designed a lean unidirectional communication protocol with software-defined detection algorithms that enable our system to send short command words while being small and easily integrated into SoFi.

The observation of marine life using robots is particularly attractive when attempting to better understand the behaviors and occurrences of animals and plants. Observatories of different levels of autonomy and biomimicry have been proposed. A cable car–mounted observatory for fish assessments (*63*) performed underwater stereoscopic imaging to observe month-long small-scale temporal patterns in fish-habitat interactions, but the system is difficult to use and not suitable for most environments. A robotic fish with a Global Positioning System and a temperature sensor demonstrated surface swimming through Wi-Fi remote control within a small tank (*64*). The aquatic hexapod AQUA (*65*) is equipped with sensors to walk over terrain in shallow waters. The AUV AMOUR V (*66*) is a low-cost thruster-based AUV capable of marine surveying and monitoring. Although it carries onboard sensors, it is less suitable for marine life observations because of its disruptive thrusters. In recent years, the development of smaller and more maneuverable AUVs such as biomimetic robots with sizes ranging from a few centimeters to a meter has been a growing field of interest (*8, 9, 67*). However, all of the studies are focused on different types of swimming locomotion and do not demonstrate deployment in the wild. We believe that biomimetic AUVs have the potential for greater efficiency, maneuverability, and stealth, which could enable minimally disruptive environmental monitoring, proximal live fish observations, and controlled interactions with marine life.

Contributions

This paper contributes to the field of robotics with the integration of an end-to-end system that locomotes in a biomimetic manner underwater, is remote-controlled, and can serve as an underwater observatory for the study of marine life. We present a biomimetic soft robotic fish that is able to swim along 3D trajectories with autonomous buoyancy control to observe the biocenosis of coral reefs in the ocean. More specifically, the contributions of this work include the first soft robotic fish prototype capable of (i) 3D controllable motion for persistent operation underwater, (ii) autonomous depth control via dive planes and a miniaturized piston-based buoyancy control unit (BCU), (iii) underwater remote control via a miniaturized end-to-end acoustic communication system, and (iv) performing at depths of 0 to 18 m, as evidenced by ocean experiments.

RESULTS

We developed SoFi, a fully embedded self-contained underwater system, that swims independently and receives high-level commands from a human diver (Fig. 1). The robot measures 0.47 m × 0.23 m × 0.18 m, weighs 1.6 kg, is neutrally buoyant, and swims for about

40 min. It propels itself by undulating its soft tail in a cyclic manner and adjusts this undulation to swim forward or turn. The tail motion is created by the cyclic flow of a displacement pump, and adjusting the relative amount of liquid pumped into each side of the tail can generate a turning motion. Vertical swimming is achieved via dive planes and a BCU. The fish is equipped with a fisheye camera at its tip to observe its environment. An acoustic transducer is also mounted in front of the rigid dorsal fin, tilted upward, to receive commands from the human-operated diver interface module.

Swimming along a 3D trajectory

The hydraulic system performed undulating tail actuation at low (0.9 Hz), medium (1.15 Hz), and high (1.4 Hz) frequencies to achieve a range of swimming speeds. The fish executed left and right turns by adjusting the baseline deflection angle of the tail around which the tail undulates. The fish performed three levels of deflections in each direction, with a maximum baseline deflection of about ±30°. Similarly, the fish could pitch its dive planes at three levels in each direction, with a maximum pitch of ±45°. A sample fish trajectory along a coral reef is shown in Fig. 2, illustrating the controlled swimming motion as it was commanded by a human diver. The fish changed direction and depth while exploring the reef, with an average swimming speed of 21.7 cm/s (±3.2 cm/s) at depths of 0 to 18 m.

We performed quantitative tests in the ocean to measure the forward and turning capabilities of the fish (Fig. 3). The average swimming speed in a straight path was 23.5 cm/s (±0.4 cm/s), equivalent to 0.5 body lengths per second. The average turning speed was 18.3 cm/s (±4.1 cm/s) on an average turning radius of 78.2 cm (±28.6 cm). Dynamic diving using the dive planes was possible within a range of ±0.9 m from its baseline depth at an average speed of about 14.0 cm/s, equivalent to 0.8 body heights per second. During the dive, we changed the robot's baseline depth within 0 to 18 m by manually adjusting attached weights. At deeper depths, the rigid foam floats experienced too much compression and inhibited upward diving.

Vertical diving capabilities using the BCU were quantified in a pool. The BCU reliably controlled depth changes of up to 2.8 m. This was repeatedly tested at different baseline depths of 1.6 to 2.7 m by adjusting magnetic weights. The average dive speed up and down was 10.6 cm/s (±1.1 cm/s), equivalent to 0.6 body heights per second. Commanding a step change in depth of 0.2 m had a 10% settling time of 17.8 s (±6.6 s). Figure 3 (top right) shows the depth profile of a vertical dive, where the robot was directed to continuously dive deeper solely by compressing the air in the piston of the BCU. The BCU responded with slight oscillations around the set depth until it settled and the next depth was
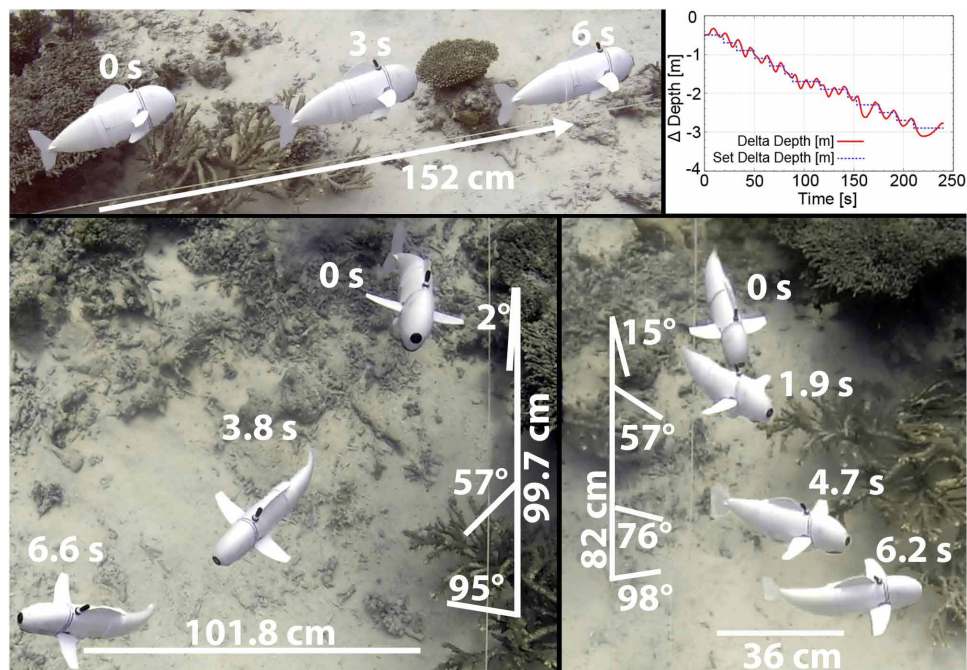

Fig. 3. Quantitative ocean experiments. Clockwise from top left: Straight swimming, vertical diving, left turn, and right turn experiments of the robotic fish.

Table 1. Communication experiments. Cumulative results of the acoustic communication during four of the six dives, spanning 2 days and averaging about 40 active minutes per dive. Note that "steady commands" are commanded states that persisted for at least 1 s. Observations were made at an average depth of 8.1 m, a maximum depth of 18 m, a range between transmitter and receiver of 0 to 10 m, and a transmit acoustic power of 137.3 dB SPL re 1 μPa.

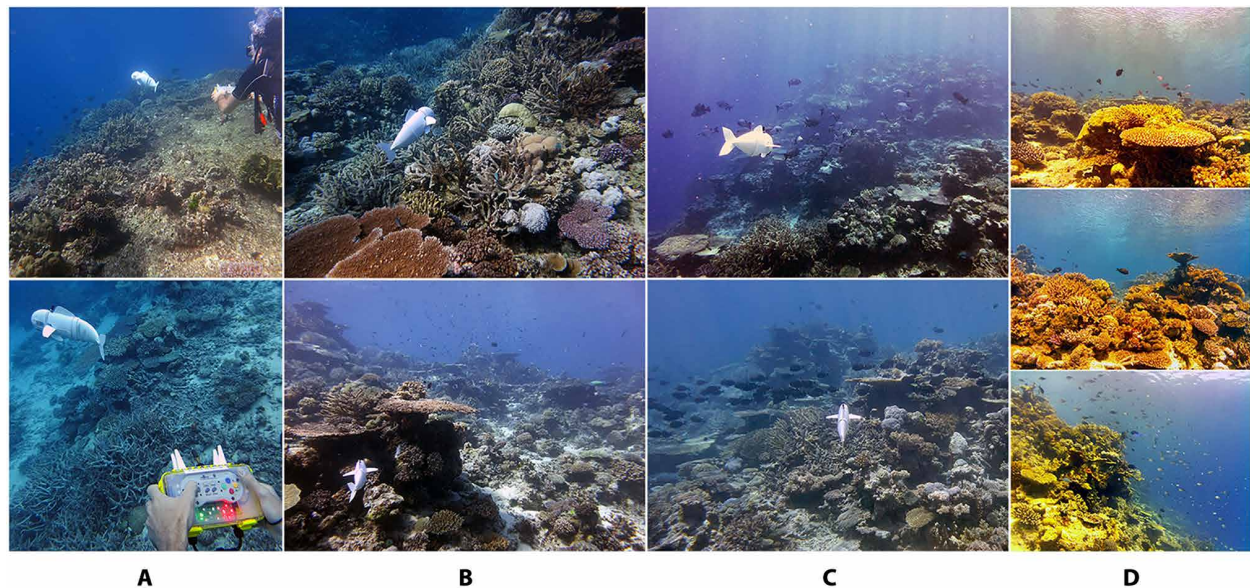|	Dive 3	Dive 4	Dive 5	Dive 6
Total commands obeyed	67	30	111	93
Total commands missed	55	62	46	57
Steady commands obeyed	55	26	75	78
Steady commands missed	25	31	7	21
Percent of steady commands obeyed	**68.8%**	**45.6%**	**91.5%**	**78.8%**
Fish timeouts (reversions to neutral state)	63	34	81	81
Percent of dive spent timed out	**12.3%**	**8.0%**	**7.3%**	**8.1%**

Fig. 4. Underwater observatory. (**A**) A diver using the acoustic communication modem to remotely control the robotic fish. (**B**) The fish exploring complex coral reef environments. (**C**) The robotic fish among marine life. (**D**) Pictures captured by the fish's onboard camera.

Fig. 5. Closeup view of marine life. (**Left**) Onboard view filming several fish passing by the lens of SoFi. (**Right**) Photo taken by a diver from further behind, showing both the robotic fish and the observed biological fish.

commanded. The two linear actuators within each of the two modules moved symmetrically to vary the buoyancy while maintaining constant pitch of the robot. Additional buoyancy control experiments are provided in fig. S5.

Human-robot interaction

The human controls SoFi remotely through a custom-designed unidirectional acoustic communication modem. This system consists of the diver interface module and the acoustic receiver, both shown in Fig. 1.

We characterized the reliability of the communication modem by transmitting a series of 200 alternating bits at a rate of 20 bits/s at varying distances and depths in a large pool. The results, shown in fig. S8, indicate that error-free communication was achieved at a depth of 1.8 m for ranges of up to about 15 m, with more than 97% of the data successfully received at 21 m, and that the effective communication range remains similar when the robot's motor is turned on. In addition, a complete sequence of 250 16-bit data words was successfully received and decoded without errors at separations of about 0.5 m in a fish tank and 10 m in a small pool.

A human diver used the diver interface module to successfully steer the robot through various complex underwater coral reef environments. The diver commanded levels of thrust, tail undulation frequency, depth/pitch, and turning angle; fig. S10 illustrates the transmitted and received commands for a single dive, and Table 1 summarizes the detection rates. During dive 5, the diver remained closer to the fish (within a few meters), and therefore, communication was more reliable. Our analysis focuses on "steady" commands, which were not immediately followed by a different command within 1 s; for example, a diver commanding a transition from lowest to highest pitch would repeatedly press the "up" arrow, resulting in transient intermediate pitch states, but only the final command state is of importance. If the fish did not receive any commands within a timeout period of about 10 s, then it would return to a neutral state and turn off the motor; this temporary silencing would then facilitate detecting fainter commands.

In the coral reef experiments (at depths ranging from 0 to 18 m), effective communication was established at a range of up to 10 m when the robot's motor was switched off and 5 m when the motor was switched on. The largest factors affecting communications were environmental complexity, noise of the fish motor, and transmission distance. Additional experiments close to the shoreline showed that, in a shallow, cluttered underwater environment, the system can communicate up to 10 m even in the presence of motor noise.

Oceanic exploration

The robotic fish has an onboard fisheye camera that allows a remote human operator to film the underwater exploration. This setup reduces the impact of the diver on the marine life being filmed. The fish continuously operated for about 40 min during each of six ~51-min dives
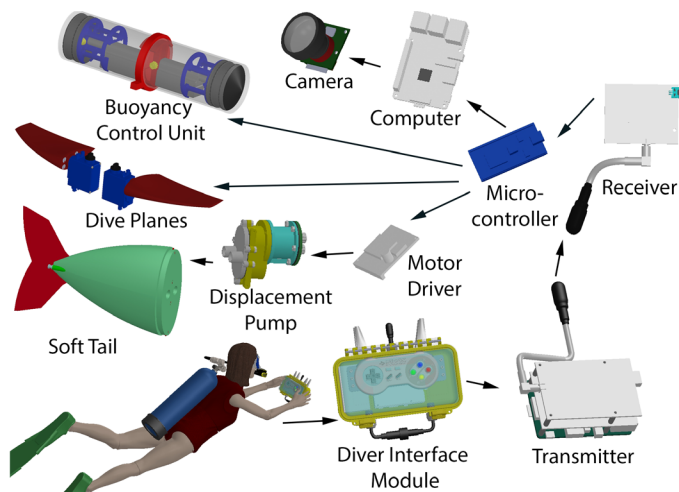
Fig. 6. Signal flow within the system. The command flow from a human diver to the robot. The diver sends acoustic commands such as thrust, left/right, and up/down as well as camera modes from the transmitter within the diver interface module. The analog signal travels several meters underwater and is then amplified by the receiver and parsed by the microcontroller. The microcontroller adjusts the pump speed, the dive plane position, the BCU, and the mode of the camera.

Fig. 7. Soft tail, pump, and BCU. (**Top**) Two views of the soft fish tail in an actuated state (left) and custom external gear pump in an exploded view (right). (**Bottom**) One of two identical BCU modules in an exploded view.

over 3 days, accumulating 240 min of controlled exploration (table S2). Each dive used a single charge of a 35–watt-hour battery. The average depth was 8.1 m, and the maximum depth was 18 m. We recorded the number of tail strokes performed for an average dive (table S3). On the basis of the average swimming speed observed during the quantitative tests, for a single dive, this would correspond to 296.8 m (±5.1 m) of straight swimming, 17.6 m (±3.9 m) of turning left, and 14.6 m (±3.3 m) of turning right. The ocean experiments showed that the robotic fish is capable of 3D controllable motions in natural environments, in the presence of currents.

During the ocean experiments, we also made preliminary observations of the robot's ability to make closeup observations of marine life and record their responses. Without the intent to imitate any specific species of biological fish, the robotic fish was colored white except for the black lens and acoustic transducer (table S1). There were several closeup encounters with underwater life during which SoFi observed fish and their interactions. We made the personal observation that SoFi did not cause other fish to flee upon these close encounters, even when within less than a meter. Figure 4 shows examples of high-level remote control by a human diver and depicts some of SoFi's explorations and observations: exploring complex coral reef environments, encountering schools of fish, and capturing images with the onboard camera. Figure 5 and movie S1 also show SoFi approaching overhanging reefs and other environments with fish swimming nearby. As the movie shows, multiple fish swim parallel to the robot a few centimeters below it and also pass a few centimeters in front of its lens. The fish did not appear to change their swimming trajectory as SoFi approached them in these cases, suggesting that SoFi has the potential to integrate into the natural underwater environment.

DISCUSSION
Conclusion
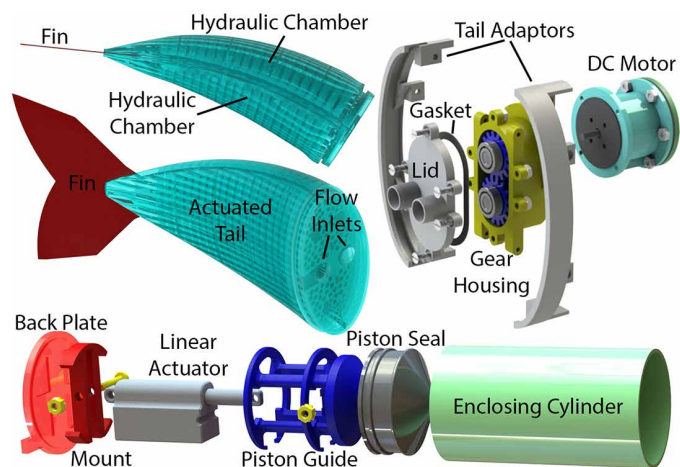We have presented an untethered soft-bodied robotic fish that demonstrates prolonged and consistent underwater remote-controlled operation. Whereas most soft robots are pneumatically powered and tethered, our hydraulically driven soft actuator enables prolonged untethered swimming over several hundred meters for 40 min. The hydraulic system can perform low- to high-frequency tail actuation to achieve a range of swimming speeds and can execute turns by adjusting the baseline deflection around which the tail undulates. Dive planes and the BCU enable vertical swimming. A camera is mounted at the tip of the robot, allowing a diver to remotely explore and capture closeup recordings of marine life and environments.

The acoustic communication system provides a compact, software-defined modulation scheme for transmitting data that is robust to substantial noise and interference from complex environments. In open-ocean coral reefs including obstacles, sources of noise, and multipath effects, SoFi was able to transmit 16-bit words once per second over distances of up to 10 m. This successfully enabled divers to send high-level commands and navigate the robotic fish, observing the marine life and exploring their surroundings.

Limitations and future steps
We demonstrated that SoFi can navigate in natural environments. The next steps are to use SoFi as an instrument to (i) study the behavior of marine life over long periods of time without human interference with the scene, (ii) study whether SoFi can be used to influence the behavior of marine life, and (iii) create robotic swarms. These research directions are enabled by SoFi and are the subject of future work.

SoFi can be created at different scales, but its swimming behavior depends on its size. Smaller robotic fish can barely overcome ocean currents and need external power (68), whereas larger robotic fish are more difficult to prototype and to handle by a diver. SoFi can currently swim up to 0.51 body lengths per second, which is comparable to other robotic fish prototypes (69, 70) but still leaves room to improve toward real fish capabilities of 2 to 10 body lengths per second (71, 72). Further optimizations of the pump system, the tail geometries, and the exterior profile of SoFi may improve swimming efficiency.

The dive planes provide only fine-tuned control at a limited depth range. Once the range is exceeded, the compression of the fish's flotation becomes so strong that inverting the pitch of the dive planes will not allow returning to the original depth; the diver must manually
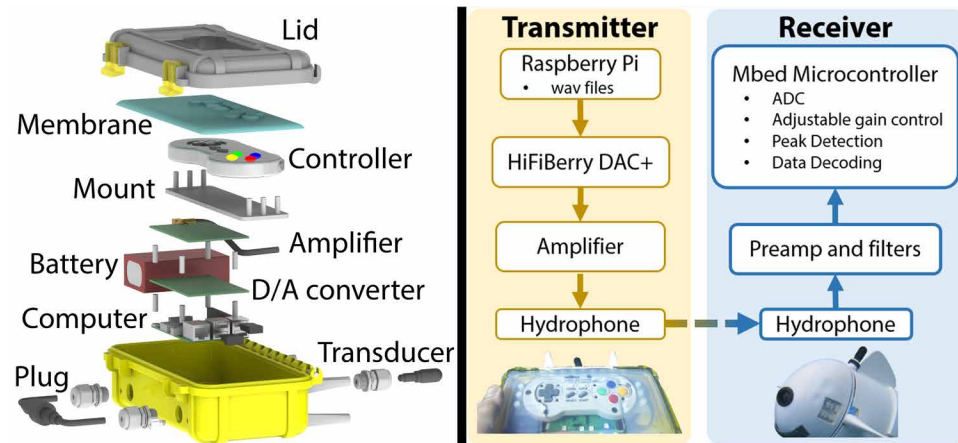
Fig. 8. Acoustic communication. (**Left**) Exploded view of the diver interface module, containing the transmitter. (**Right**) Schematic view of the transmitter and receiver pipelines.

adjust the weight during the dive to change to another depth range. Using asynchronous control of the BCU modules would enable increased pitch control (see fig. S4 for details), although the BCU is still limited in its diving speed and range. The speed and range can be increased by enlarging the body to allow for larger dive planes or BCU pistons while balancing against the trade-off of increased drag. Upgrading the tail design to four instead of two fluidic chambers, with one chamber per quadrant, would also allow steering in the vertical direction through biased undulation of the tail in the vertical plane.

Improving the acoustic modem could allow a diver to be further away. Optimizing the modulation parameters, implementing different protocols such as frequency hopping, refining the transducer and amplifier circuitry, and reducing the motor noise could increase data rates and detector robustness. In addition, the modem can be extended to control multiple robots or to be bidirectional and provide the diver with real-time feedback.

The integrated camera enables more autonomous surveying capabilities (*73*). Monocular self-localization would enable the fish to build maps of the underwater environment and explore it further. Instead of using acoustic communication for lower-level settings such as thrust and depth, a diver could remotely command higher-level mission parameters such as regions to explore or specific marine life to follow.

There are many potential future applications of the robotic fish described in this paper in the emerging field of ethorobotics (*1, 2*). We are inspired by previous work that considered robot-animal interactions, including research on robot-cockroach societies (*74*), remote-controlled cow gathering (*75*), pet care robots (*76*), honeybee robots (*77*), and guinea fowl (*78*). More recently, studies in small fish tanks began to specifically investigate interactions between robotic fish lures and natural fish, such as golden shiners (*5, 6*), zebrafish (*31–33, 79, 80*), or Siamese fighting fish (*35*). This previous work considers controlled studies in laboratory environments, conducted in tanks with unactuated fish replicas or primitive robotic fish prototypes with servo-actuated tails. These previous studies showed that the appearance or biomimetic locomotion of the robotic device does not ensure integration within a school of fish because acceptance depends on multiple signals. It was also found that a robotic fish can be differently perceived in terms of attractiveness by real fish (*32, 35, 79, 81*). These as-

pects should be taken into account when designing robot-fish studies with our prototype in the future.

In contrast to previous robot-fish studies, the robot prototype presented in this work provides the opportunity to perform studies of the biocenosis of coral reefs and other marine environments within natural habitats. In the future, researchers could use the soft robotic fish described in this paper and easily change its size, color, and shape to emulate various types of fish with different dynamic behaviors. The integrated camera and the ability to remotely control the robot in three dimensions at a variety of depths allow the system to observe and approach marine life.

The soft fish presented in this paper can also be rapidly fabricated to create a swarm of robotic fish. Such a swarm could enable studies of schools of fish and their interactions in the presence of varying ocean dynamics (*82–85*).

MATERIALS AND METHODS
The objective of this study is to show that we can create a soft robotic fish that uses undulating motion to swim in the ocean and explore underwater life and structures.

System architecture
The full system and its major subcomponents are shown in Fig. 1. The nose of the fish is a waterproof housing for the fisheye camera, microcontroller, computer, motor driver, wireless communication electronics, inertial measurement unit, and depth sensor. The housing is 3D-printed and waterproofed by brush-coating it with preheated epoxy paint and subsequent degassing. Behind the nose is the dive plane assembly, consisting of two individually controllable dive plane units. Each unit consists of a dive plane directly mounted onto the lever arm of a waterproof servo motor. The dive plane assembly is mounted to the end of the gear pump's DC motor. The motor and gear pump unit are directly attached to the soft fish tail. Underneath the gear pump motor is a lithium polymer battery to power all components. Above the gear pump is the BCU. The mass of the complete assembly was slightly adjusted to make it almost neutrally buoyant using internal rigid urethane foam chambers and additional magnetic weights placed underneath the robotic fish.

The flow of commands within the system is depicted in Fig. 6. The diver commands a change to the fish state via the gamepad controller within the diver interface module. The command is encoded into an acoustic signal transmitted via the acoustic transducer to the amplifying receiver within the fish. The microcontroller decodes the received command and adjusts its state accordingly. Changes to the swimming speed or turning motion change the behavior of the displacement pump and therefore the soft tail undulation. Changes in pitch or depth, depending on the mode, are sent to the servos of the dive planes or the BCU. Changes to the video recording state are forwarded to the single-board computer, which records from the fisheye camera.

Soft body for undulating locomotion

The fish achieves undulating locomotion via a hydraulically actuated soft fish tail with two internal cavities. The soft fish tail, shown in Fig. 7, is a fluidic elastomer actuator (39, 86, 87). The design mimics the rear portion of a fish, encompassing the posterior peduncle and the caudal fin. The tail can continuously bend along its vertical center constraint layer by fluidic actuation of two lateral cavity structures. The inextensible and stiffer center constraint layer splits the tail evenly along a vertical plane. An actuator consists of evenly spaced ribs with hollow sections in between, connected by a center channel and accessible by a front inlet. The rib structure allows for expansion or contraction of the thin exterior skin under positive or negative fluidic pressure, respectively. These expanding or contracting motions bend the inextensible center constraint layer. The rib structure is evenly spread along the fin, leading to a continuous flexing of the whole body under fluidic pressure. The inherent elasticity of the body forces it back into its neutral state after each pulse of actuation. A fluidic flow alternating into each lateral cavity structure leads to a complex undulating motion of the soft body and enables swimming.

The fabrication of the soft body with its integrated constraint layers and posterior fins is realized through a lost-wax fabrication process. The interior cavity of the body is realized through a lost-wax core (fig. S1). The constraint layers are laser-cut, and the surrounding molds are 3D-printed. The wax cores and the constraint layers, which also act as the posterior fins, are assembled together into a mold (fig. S2). The soft silicone elastomer and low-density glass bubbles are mixed at a mass ratio of 40:1 to achieve a desired rubber density of 0.94 g/cm^3. This mix is filled into the cavity and allowed to cure. Heating the resulting body in an oven and then in a water bath removes the interior wax body and creates the soft body.

Cyclic hydraulic actuation

The soft tail is actuated by a hydraulic pump at a desired undulation frequency and amplitude. The outlets of the hydraulic pump are directly attached to the soft body to allow for water movement between the two inner cavities in a closed-loop fashion. Alternating the flow direction leads to a flexing actuation of the soft body in a side-to-side manner, propelling the robot forward. The soft tail has removable plugs at the caudal fin, which are initially removed, so water can fill the actuation chambers by running the self-priming gear pump at a low frequency for a short duration. After all air has been removed, the plugs are inserted to seal the chambers.

We dimensioned the custom-designed pump (fig. S3) and its attached motor based on the maximum pressure required and the volumetric flow rate. We estimated the effective volumetric flow rate based on the displaced volume of fluid for a single static deflection and the desired flapping frequency. Initial values for the desired flapping frequency and the amplitude of the soft tail were determined based on previous studies on self-propelling foils driven by an external actuator (88, 89). A custom pump, its attached motor, and a waterproof housing were then specified, designed, and built. The effectiveness of six different self-contained designs based on a centrifugal pump, a flexible impeller pump, an external gear pump, and rotating valves was compared. These hydraulic actuation systems combined with the soft tail were then measured at low and high oscillation frequencies. The propulsive force, deflection characteristics of the soft tail, acoustic noise of the pump, and overall efficiency of the system were recorded. A brushless, centrifugal pump combined with a custom-printed rotating valve performed most efficiently at both test frequencies, pro-ducing sufficiently large cyclic body deflections and the least acoustic noise. An external gear pump design produced the largest body deflection and therefore the best swimming performance but consumed an order of magnitude more power and produced higher noise levels. A detailed study of the various actuation systems is provided in (90). We chose an external gear pump (Fig. 7) for the fully integrated robotic fish because of its better swimming performance, lower part count, and easier controllability.

The motor controller operates the motor attached to the pump through a trapezoidal voltage profile, alternating from positive to negative voltages after each half-cycle. This profile rotates the motor shaft back and forth, causing the pump to create a cyclic hydraulic flow. Asymmetrically varying the flow intensity for each half-phase can enable yaw control by creating a pressure bias in the tail.

Depth control

The depth of SoFi is controlled by dive planes or the BCU. The dive planes, shown in Fig. 1, allow the diver to finely control the robot's change in depth through dynamic diving for limited deviations from its baseline depth before a buoyancy adjustment is needed. Manually adding or removing magnetic weights attached to the bottom of the robot adjusts the neutral depth level. This allows the diver to operate the robot over a larger depth range.

In addition, the diver can remotely adjust the neutral buoyancy of the robot using the BCU. The BCU, shown in Fig. 1, can simultaneously control the buoyancy and pitch of the robot. The mechanical design of the BCU comprises two mirroring volume control modules in the form of two pistons. The BCU is symmetrically oriented at the robot's center of buoyancy. An exploded view of a single unit is presented in Fig. 7. A single unit contains a micro linear actuator with potentiometer feedback (PQ12, Actuonix, Victoria, Canada) that sits within a watertight cylinder and moves a piston. A closed-loop proportional-integral-derivative (PID) controller with pressure feedback from an integrated pressure sensor is used to drive the volume-changing actuators. Ascent, descent, and hovering can be achieved over several meters by symmetrically controlling the pistons. The pitch can also be modified by asymmetrically controlling the two pistons (fig. S4).

The BCU's performance was quantitatively evaluated in an indoor swimming pool with a depth of 4.2 m. There were no substantial disturbances in the environment except for the pool circulation and swimmers in adjacent lanes. The gains of the PID controller were estimated by averaging the results of two frequency response tests (91). Before the start of each trial, the robot's weight was adjusted for neutral buoyancy at a desired baseline depth. Desired depth values were then commanded as a step function. Once a set depth was held for 4 s within an error margin of 10%, the next depth level was commanded. The robot's microcontroller continuously logged depth by reading a pressure sensor. Each run started at a different depth to investigate varying baselines. We measured the depth, speed, duty cycles, and error.

Underwater communication
Acoustic modem design

We designed a compact unidirectional acoustic communication modem to allow SoFi to support remote-controlled operation. The diver interface module (Fig. 8, left) contains the transmitter and allows a diver to issue commands, whereas the receiver is embedded within SoFi's head. Tight volumetric constraints made accommodating existing underwater modem designs impractical. Thus, we implemented

a new low-power, low-cost, software-defined acoustic modem, represented schematically in Fig. 8 on the right and described in detail in (12).

The acoustic modem's transmitter is housed in the diver interface module, which incorporates an oil-filled rigid outer shell (22 cm by 22 cm by 6 cm) with a transparent flexible membrane on one face. The membrane, a soft cast-molded silicone rubber (SORTA-Clear 40, Smooth-On), retains nonconductive mineral oil within the housing and allows for pressure equalization underwater. The flexibility and molded shape of the membrane allow the control buttons within the module to be pressed by the diver when selecting a desired fish state. These commands are read by a Raspberry Pi single-board computer via Universal Serial Bus and are encoded as a specific sequence of ultrasonic acoustic tones, which are then converted to audio signals by a digital-to-analog converter (HiFiBerry). The analog signals are amplified via a Class G differential audio amplifier (MAX9788) and are then impedance-matched to the output ceramic transducer (Aquarian Scientific AS-1 hydrophone) via a step-up transformer (Pico Electronics 32146). The hydrophone has a transmit sensitivity of 116 dB relative to (re) 1 V/μPa (1 voltage root mean square input at 1-m range) at 30 kHz and was driven at 32.8 V peak-to-peak, yielding a transmit sound pressure level (SPL) of 137.3 dB re 1 μPa.

The modem's receiver, housed within an oil-filled chamber in SoFi's head (see Fig. 1), occupies less than 30 cm^3. Audio signals are transduced by a hydrophone (Aquarian Scientific AS-1) with a voltage-mode receive sensitivity of −207 dB re 1 V/μPa, amplified and filtered by a custom Junction Field Effect Transistor preamplifier with a 17-dB gain, filtered and amplified by a band-pass filter with a 20- to 40-kHz passband and a 40-dB gain, and digitized by an Mbed microcontroller. A variable-gain amplifier controlled by the Mbed allows dynamic signal equalization with a gain from 0 to 40 dB. Modulation and demodulation are both defined in software for versatility, facilitating alternate modulation protocol implementations. The receiver consumes 815 mW, with the Mbed using about 740 mW of that power.

Communication frequencies were chosen by considering typical ranges of human hearing, frequency-dependent attenuation in underwater channels (56), Doppler effects, SoFi's motor noise, the microcontroller's sampling capabilities, parameters of the receiver's detection algorithm, expected sources of environmental noise such as wind and waves (92, 93), and marine life. Noise produced by fish is typically below 10 kHz (94), and the hearing ranges of common aquatic species decay significantly above 10 kHz (95, 96), although some cetaceans and pinnipeds can hear well above this range (4). Taking into account all of these considerations, 36 kHz was chosen for a logical 0 and 30 kHz was chosen for a logical 1.

Considering the design constraints, a modulation scheme that could be efficiently implemented in software on a microcontroller while still being robust to multipath effects and Doppler shifts was designed. It uses pulse-based frequency-shift keying and a computationally efficient software-defined demodulation approach leveraging the Goertzel algorithm (97) and a custom dynamic peak detection algorithm. The chosen parameters support 2048 distinct messages with a data rate of one message per second at 20 bits/s. Further details on the algorithm can be found in (12).

The desired fish state, encoded as a 16-bit word, is transmitted from the controller once per second. Each command describes a desired state of the fish including tail oscillation frequency (2 bits), oscillation amplitude (2 bits), pitch or depth (3 bits), yaw (3 bits), and video recording (1 bit). These 11 bits are expanded to a 16-bit word using a [15,11] Hamming encoding with an additional parity bit. This vocabulary of commands can then be used to remotely control the fish.

Acoustic modem testing

We evaluated the acoustic modem in a pool, a fish tank, and the ocean. The system was first evaluated in a tank (1.2 m × 0.3 m × 0.45 m) and pool (23 m × 12.5 m × 2.2 to 4.2 m) to test the modem under controlled conditions. These environments facilitate multipath reflections due to the enclosed configuration, hard walls, and shallow depth, approximating the types of interference observed in open-ocean deployments.

As described in more detail in the Supplementary Materials, tests were performed during development to choose parameters of the modulation scheme and decoding algorithm. Then, to evaluate the communication reliability of the completed modem, we transmitted a series of 200 alternating bits at a rate of 20 bits/s over a sequence of increasing distances and depths. For each transmission, the percentage of bits correctly decoded by the receiver and the longest error-free segment of received bits were extracted. After evaluating single-bit transmissions, transmissions of complete words were investigated by sending a predefined series of 250 16-bit data words using 50 ms for each bit and 200 ms between words. The correctness of the decoded sequence was then measured. Last, the complete modem integrated within SoFi was used in the open ocean to evaluate performance in real-world operations.

Open-ocean experiments

We tested the complete system in the open ocean, with a diver remotely adjusting the fish's state and navigating it to points of interest in a complex underwater environment. Six dives were conducted over the course of 3 days, exploring the Somosomo Strait in Taveuni, Fiji (see table S2 for details). This location offers numerous coral reef environments with varying tidal conditions, allowing SoFi to be evaluated in real-world conditions where the interactions of marine life and the biocenosis of coral reefs can be studied.

The robot conducted about 40 min of continuous observation during each dive, totaling about 240 min of controlled exploration at an average depth of 8.1 m and a maximum depth of 18 m. We performed an additional 90 min of preparatory swim tests in shallow ocean waters to test the control system, communication, and video recording. All of these tests evaluated the effectiveness of SoFi's biomimetic actuation and the usability of the acoustic communication interface for remote control. The distance between the operator and SoFi was typically between 1 and 10 m, and the transmit power of the acoustic modem was 137.3 dB SPL re 1 μPa. The robot's trajectories along the reefs and following other fish were documented by two or more divers using GoPro Hero 3, Canon PowerShot S100, and Olympus Tough TG-1 cameras from a distance of several meters.

Qualitative observations were made during five of the dives, during which SoFi explored the coral reef environments. The magnetic weights were adjusted at the beginning of each dive for neutral buoyancy and then the robot was continuously operated via the acoustic modem. The distance between controller and robot was varied to understand the effective communication range. The fish was steered throughout the coral reefs, going as close as possible to interesting environmental features and marine life. Such dives provided qualitative observations of SoFi's swimming capabilities in constrained and unconstrained areas, of the acoustic communication reliability, and of the effect that SoFi has on nearby fish.

In addition, one dive was dedicated to performing quantitative swimming tests on the ocean floor at a baseline depth of about 7 m. We installed several premeasured ropes to define a reference volume (4 m × 4 m × 1 m) for measuring and filming the robot's ability to swim straight, turn right, turn left, dive up, and dive down. We performed three trials for each ability. During all trials, the thrust was set to maximum and the undulation frequency was set to medium (1.15 Hz). For right and left turns, the yaw was set to ±30° and the dive planes were set to neutral. For up or down swimming, the dive planes were adjusted to ±45° and yaw was set to neutral. Yaw and pitch were both neutral for straight swimming. At the beginning of each trial, a diver repositioned the fish to its starting position at the center of one of the bounding planes of the reference volume and then released the fish without pushing it. This diver also took notes during trials. A second diver commanded the desired fish state from the starting position. Two additional divers filmed the trials from the side and top, standing or floating at the boundary of the reference volume.

Throughout all sessions, the diver interface module transmitted the desired fish state once per second using a bitrate of 20 bits/s. By recording logs of commands on both the transmitter and receiver, the percentage of commands successfully received and executed by SoFi could be extracted. In addition, qualitative observations regarding achievable communication distances, the effect of real-world obstacles such as coral reefs on transmission reliability, the effect of ambient noise such as from marine life, and the effect of the system on surrounding organisms were made.

We estimated the number of tail strokes at various combinations of thrust and yaw using the logs of the executed fish states. Using the highest commanded undulation frequency, we estimated a conservative total stroke duration. We then weighted according to thrust level and used the average speed from the quantitative tests to estimate the swimming distance.

SUPPLEMENTARY MATERIALS

robotics.sciencemag.org/cgi/content/full/3/16/eaar3449/DC1
Materials and Methods
Fig. S1. Wax core fabrication.
Fig. S2. Tail fabrication.
Fig. S3. External gear pump.
Fig. S4. Buoyancy control system.
Fig. S5. Additional buoyancy control experiments.
Fig. S6. Acoustic reflections.
Fig. S7. Motor's broad spectrum noise.
Fig. S8. Acoustic range tests.
Fig. S9. Performance of tone detection algorithm.
Fig. S10. Ocean communication tests.
Table S1. Color measurements of exposed parts.
Table S2. Dive summaries.
Table S3. Tail strokes.
Movie S1. Underwater experiments.

REFERENCES AND NOTES

1. J. Krause, A. F. T. Winfield, J.-L. Deneubourg, Interactive robots in experimental biology. *Trends Ecol. Evol.* **26**, 369–375 (2011).
2. Á. Miklósi, L. Gerencsér, Potential application of autonomous and semiautonomous robots in the study of animal behaviour, in *2012 IEEE 3rd International Conference on Cognitive Infocommunications (CogInfoCom)* (IEEE, 2012), pp. 759–762.
3. R. Bogue, Underwater robots: A review of technologies and applications. *Ind. Rob.* **42**, 186–191 (2015).
4. B. L. Southall, A. E. Bowles, W. T. Ellison, J. J. Finneran, R. L. Gentry, C. R. Greene Jr., D. Kastak, D. R. Ketten, J. H. Miller, P. E. Nachtigall, W. J. Richardson, J. A. Thomas, P. L. Tyack, Overview. *Aquat. Mamm.* **33**, 411–414 (2007).
5. S. Marras, M. Porfiri, Fish and robots swimming together: Attraction towards the robot demands biomimetic locomotion. *J. R. Soc. Interface* **9**, 1856–1868 (2012).
6. S. Butail, N. Abaid, S. Macrì, M. Porfiri, Fish–robot interactions: Robot fish in animal behavioral studies, in *Robot Fish*, R. Du, Z. Li, K. Youcef-Toumi, P. Valdivia y Alvarado, Eds. (Springer, 2015), *Springer Tracts in Mechanical Engineering*, pp. 359–377.
7. L. Hines, K. Petersen, G. Z. Lum, M. Sitti, Soft actuators for small-scale robotics. *Adv. Mater.* **29** (2017).
8. W.-S. Chu, K.-T. Lee, S.-H. Song, M.-W. Han, J.-Y. Lee, H.-S. Kim, M.-S. Kim, Y.-J. Park, K.-J. Cho, S.-H. Ahn, Review of biomimetic underwater robots using smart actuators. *Int. J. Precis. Eng. Manuf.* **13**, 1281–1292 (2012).
9. A. Raj, A. Thakur, Fish-inspired robots: Design, sensing, actuation, and autonomy—A review of research. *Bioinspir. Biomim.* **11**, 031001 (2016).
10. A. D. Marchese, C. D. Onal, D. Rus, Autonomous soft robotic fish capable of escape maneuvers using fluidic elastomer actuators. *Soft Robot.* **1**, 75–87 (2014).
11. R. K. Katzschmann, A. D. Marchese, D. Rus, Hydraulic autonomous soft robotic fish for 3D swimming, in *Experimental Robotics: The 14th International Symposium on Experimental Robotics*, M. A. Hsieh, O. Khatib, V. Kumar, Eds. (Springer International Publishing, 2014), vol. 109, pp. 405–420.
12. J. DelPreto, R. K. Katzschmann, R. MacCurdy, D. Rus, A compact acoustic communication module for remote control underwater, in *WUWNET'15: Proceedings of the 10th International Conference on Underwater Networks & Systems* (ACM, 2015), pp. 1–7.
13. A. M. Wilson, J. C. Lowe, K. Roskilly, P. E. Hudson, K. A. Golabek, J. W. McNutt, Locomotion dynamics of hunting in wild cheetahs. *Nature* **498**, 185–189 (2013).
14. S. Seok, A. Wang, M. Y. Chuah, D. J. Hyun, J. Lee, D. M. Otten, J. H. Lang, S. Kim, Design principles for energy-efficient legged locomotion and implementation on the MIT cheetah robot. *IEEE ASME Trans. Mechatron.* **20**, 1117–1129 (2015).
15. D. N. Beal, F. S. Hover, M. S. Triantafyllou, J. C. Liao, G. V. Lauder, Passive propulsion in vortex wakes. *J. Fluid Mech.* **549**, 385–402 (2006).
16. J. M. Anderson, N. K. Chhabra, Maneuvering and stability performance of a robotic tuna. *Integr. Comp. Biol.* **42**, 118–126 (2002).
17. V. Pavlov, B. Rosental, N. F. Hansen, J. M. Beers, G. Parish, I. Rowbotham, B. A. Block, Hydraulic control of tuna fins: A role for the lymphatic system in vertebrate locomotion. *Science* **357**, 310–314 (2017).
18. D. Rus, M. T. Tolley, Design, fabrication and control of soft robots. *Nature* **521**, 467–475 (2015).
19. D. Trivedi, C. D. Rahn, W. M. Kier, I. D. Walker, Soft robotics: Biological inspiration, state of the art, and future research. *Appl. Bionics. Biomech.* **5**, 99–117 (2008).
20. S. Kim, C. Laschi, B. Trimmer, Soft robotics: A bioinspired evolution in robotics. *Trends Biotechnol.* **31**, 287–294 (2013).
21. C. Laschi, B. Mazzolai, M. Cianchetti, Soft robotics: Technologies and systems pushing the boundaries of robot abilities. *Sci. Robot.* **1**, eaah3690 (2016).
22. A. D. Marchese, C. D. Onal, D. Rus, Towards a self-contained soft robotic fish: On-board pressure generation and embedded electro-permanent magnet valves, in *Experimental Robotics: The 13th International Symposium on Experimental Robotics*, J. P. Desai, G. Dudek, O. Khatib, V. Kumar, Eds. (Springer International Publishing, 2013), vol. 88 of *Springer Tracts in Advanced Robotics*, pp. 41–54.
23. P. Phamduy, M. Vazquez, A. Rizzo, M. Porfiri, Miniature underwater robotic fish for animal-robot interactions, in *ASME 2016 Dynamic Systems and Control Conference* (ASME, 2016), vol. 2, p. V002T17A009.
24. K. Suzumori, S. Endo, T. Kanda, N. Kato, H. Suzuki, A bending pneumatic rubber actuator realizing soft-bodied manta swimming robot, in *International Conference on Robotics and Automation* (IEEE, 2007), pp. 4975–4980.
25. A. Cloitre, B. Arensen, N. M. Patrikalakis, K. Youcef-Toumi, P. V. Y. Alvarado, Propulsive performance of an underwater soft biomimetic batoid robot, in *The Twenty-fourth International Ocean and Polar Engineering Conference* (International Society of Offshore and Polar Engineers, 2014), vol. 3, pp. 326–333.
26. T. Li, G. Li, Y. Liang, T. Cheng, J. Dai, X. Yang, B. Liu, Z. Zeng, Z. Huang, Y. Luo, T. Xie, W. Yang, Fast-moving soft electronic fish. *Sci. Adv.* **3**, e1602045 (2017).
27. C. Stefanini, S. Orofino, L. Manfredi, S. Mintchev, S. Marrazza, T. Assaf, L. Capantini, E. Sinibaldi, P. Grillner, P. Wallén, P. Dario, A novel autonomous, bioinspired swimming robot developed by neuroscientists and bioengineers. *Bioinspir. Biomim.* **7**, 025001 (2012).
28. L. Manfredi, T. Assaf, S. Mintchev, S. Marrazza, L. Capantini, S. Orofino, L. Ascari, S. Grillner, P. Wallén, Ö. Ekeberg, C. Stefanini, P. Dario, A bioinspired autonomous swimming robot as a tool for studying goal-directed locomotion. *Biol. Cybern.* **107**, 513–527 (2013).
29. M. Calisti, M. Giorelli, G. Levy, B. Mazzolai, B. Hochner, C. Laschi, P. Dario, An octopus-bioinspired solution to movement and manipulation for soft robots. *Bioinspir. Biomim.* **6**, 036002 (2011).
30. F. G. Serchi, A. Arienti, I. Baldoli, C. Laschi, An elastic pulsed-jet thruster for Soft Unmanned Underwater Vehicles, in *2013 IEEE International Conference on Robotics and Automation (ICRA)* (IEEE, 2013), pp. 5103–5110.

31. G. Polverino, N. Abaid, V. Kopman, S. Macrì, M. Porfiri, Zebrafish response to robotic fish: Preference experiments on isolated individuals and small shoals. *Bioinspir. Biomim.* **7**, 036019 (2012).

32. V. Cianca, T. Bartolini, M. Porfiri, S. Macrì, A robotics-based behavioral paradigm to measure anxiety-related responses in zebrafish. *PLOS ONE* **8**, e69661 (2013).

33. T. Ruberto, V. Mwaffo, S. Singh, D. Neri, M. Porfiri, Zebrafish response to a robotic replica in three dimensions. *R. Soc. Open Sci.* **3**, 160505 (2016).

34. F. Bonnet, Y. Kato, J. Halloy, F. Mondada, Infiltrating the zebrafish swarm: Design, implementation and experimental tests of a miniature robotic fish lure for fish–robot interaction studies. *Artif. Life Robot.* **21**, 239–246 (2016).

35. D. Romano, G. Benelli, E. Donati, D. Remorini, A. Canale, C. Stefanini, Multiple cues produced by a robotic fish modulate aggressive behaviour in Siamese fighting fishes. *Sci. Rep.* **7**, 4667 (2017).

36. Y. Xia, G. M. Whitesides, Soft lithography. *Annu. Rev. Mater. Sci.* **28**, 153–184 (1998).

37. J. G. Cham, S. A. Bailey, J. E. Clark, R. J. Full, M. R. Cutkosky, Fast and robust: Hexapedal robots via shape deposition manufacturing. *Int. J. Rob. Res.* **21**, 869–882 (2002).

38. R. Deimel, O. Brock, A compliant hand based on a novel pneumatic actuator, in *2013 IEEE International Conference on Robotics and Automation (ICRA)* (IEEE, 2013), pp. 2047–2053.

39. A. D. Marchese, R. K. Katzschmann, D. Rus, A recipe for soft fluidic elastomer robots. *Soft Robot.* **2**, 7–25 (2015).

40. R. MacCurdy, R. Katzschmann, Y. Kim, D. Rus, Printable hydraulics: A method for fabricating robots by 3D co-printing solids and liquids, in *2016 IEEE International Conference on Robotics and Automation (ICRA)* (IEEE, 2016), pp. 3878–3885.

41. R. MacCurdy, J. Lipton, S. Li, D. Rus, Printable programmable viscoelastic materials for robots, in *2016 IEEE/RSJ International Conference on Intelligent Robots and Systems (IROS)* (IEEE, 2016), pp. 2628–2635.

42. M. Wehner, M. T. Tolley, Y. Mengüç, Y.-L. Park, A. Mozeika, Y. Ding, C. Onal, R. F. Shepherd, G. M. Whitesides, R. J. Wood, Pneumatic energy sources for autonomous and wearable soft robotics. *Soft Robot.* **1**, 263–274 (2014).

43. D. McFarland, I. Gilhespy, E. Honary, DIVEBOT: A diving robot with a whale-like buoyancy mechanism. *Robotica* **21**, 385–398 (2003).

44. K. Shibuya, Y. Kado, S. Honda, T. Iwamoto, K. Tsutsumi, Underwater robot with a buoyancy control system based on the spermaceti oil hypothesis, in *2006 IEEE/RSJ International Conference on Intelligent Robots and Systems* (IEEE, 2006), pp. 3012–3017.

45. J. Laine, S. A. Nichols, D. K. Novick, P. D. O'Malley, D. Copeland, A. A. Arroyo, M. C. Nechyba, SubjuGator: A Highly Maneuverable, Intelligent Underwater Vehicle (2015); www.mil.ufl.edu/publications/fcrar00/subjugator.pdf.

46. S. Guo, K. Sugimoto, S. Hata, J. Su, K. Oguro, A new type of underwater fish-like microrobot, in *2000 IEEE/RSJ International Conference on Intelligent Robots and Systems* (IEEE, 2000), vol. 2, pp. 867–872.

47. R. E. Davis, C. C. Eriksen, C. P. Jones, Autonomous buoyancy-driven underwater vehicle gliders, in *Technology and Applications of Autonomous Underwater Vehicles*, G. Griffiths, Ed. (Taylor & Francis, 2002), pp. 37–62.

48. C. Detweiler, S. Sosnowski, I. Vasilescu, D. Rus, Saving energy with buoyancy and balance control for underwater robots with dynamic payloads, in *Experimental Robotics*, O. Khatib, V. Kumar, G. J. Pappas, Eds. (Springer, 2009), vol. 54 of the *Springer Tracts in Advanced Robotics*, pp. 429–438.

49. A. Cloitre, V. Subramaniam, N. Patrikalakis, P. Valdivia y. Alvarado, Design and control of a field deployable Batoid Robot, in *2012 4th IEEE RAS & EMBS International Conference on Biomedical Robotics and Biomechatronics (BioRob)* (IEEE, 2012), pp. 707–712.

50. L. Liu, S. Zhou, J.-H. Cui, Prospects and problems of wireless communication for underwater sensor networks. *Proc. Int. Wirel. Commun. Mob. Comput. Conf.* **8**, 977–994 (2008).

51. X. Che, I. Wells, G. Dickers, P. Kear, X. Gong, Re-evaluation of RF electromagnetic communication in underwater sensor networks. *IEEE Commun. Mag.* **48**, 143–151 (2010).

52. I. Vasilescu, K. Kotay, D. Rus, M. Dunbabin, P. Corke, Data collection, storage, and retrieval with an underwater sensor network, in *Proceedings of the 3rd International Conference on Embedded Networked Sensor Systems (SenSys 2005)* (ACM, 2005), pp. 154–165.

53. M. Doniec, M. Angermann, D. Rus, An end-to-end signal strength model for underwater optical communications. *IEEE J. Oceanic Eng.* **38**, 743–757 (2013).

54. M. Doniec, I. Topor, M. Chitre, D. Rus, Autonomous, localization-free underwater data muling using acoustic and optical communication, in *Experimental Robotics*, J. P. Desai, G. Dudek, O. Khatib, V. Kumar, Eds. (Springer, 2013), pp. 841–857.

55. M. Chitre, S. Shahabudeen, M. Stojanovic, Underwater acoustic communications and networking: Recent advances and future challenges. *Mar. Technol. Soc. J.* **42**, 103–116 (2008).

56. M. Stojanovic, J. Preisig, Underwater acoustic communication channels: Propagation models and statistical characterization. *IEEE Commun. Mag.* **47**, 84–89 (2009).

57. P. Lacovara, High-bandwidth underwater communications. *Mar. Technol. Soc. J.* **42**, 93–102 (2008).

58. M. Johnson, D. Herold, J. Catipovic, The design and performance of a compact underwater acoustic network node, in *Proceedings* of the *Oceans Engineering for Today's Technology and Tomorrow's Preservation (OCEANS'94)* (IEEE, 1994), vol. 3, pp. III–467.

59. L. Freitag, M. Johnson, M. Grund, S. Singh, J. Preisig, Integrated acoustic communication and navigation for multiple UUVs, in *OCEANS 2001 MTS/IEEE Conference and Exhibition* (IEEE, 2001), vol. 4, pp. 2065–2070.

60. I. F. Akyildiz, D. Pompili, T. Melodia, Underwater acoustic sensor networks: Research challenges. *Ad Hoc Netw.* **3**, 257–279 (2005).

61. M. S. Martins, N. Pinto, G. Rocha, J. Cabral, S. L. Mendez, Development of a 1 Mbps low power acoustic modem for underwater communications, in *2014 IEEE International Ultrasonics Symposium (IUS)* (IEEE, 2014), pp. 2482–2485.

62. A. Sánchez, S. Blanc, P. Yuste, A. Perles, J. J. Serrano, An ultra-low power and flexible acoustic modem design to develop energy-efficient underwater sensor networks. *Sensors* **12**, 6837–6856 (2012).

63. P. Fischer, A. Weber, G. Heine, H. Weber, Habitat structure and fish: Assessing the role of habitat complexity for fish using a small, semiportable, 3-D underwater observatory. *Limnol. Oceanogr. Methods* **5**, 250–262 (2007).

64. X. Tan, D. Kim, N. Usher, D. Laboy, J. Jackson, A. Kapetanovic, J. Rapai, B. Sabadus, X. Zhou, An autonomous robotic fish for mobile sensing, in *2006 IEEE/RSJ International Conference on Intelligent Robots and Systems* (IEEE 2006), pp. 5424–5429.

65. C. Georgiades, A. German, A. Hogue, H. Liu, C. Prahacs, A. Ripsman, R. Sim, L.-A. Torres, P. Zhang, M. Buehler, G. Dudek, M. Jenkin, E. Milios, AQUA: An aquatic walking robot, in *2004 IEEE/RSJ International Conference on Intelligent Robots and Systems (IROS)* (IEEE, 2004), vol. 4, pp. 3525–3531.

66. I. Vasilescu, C. Detweiler, M. Doniec, D. Gurdan, S. Sosnowski, J. Stumpf, D. Rus, AMOUR V: A hovering energy efficient underwater robot capable of dynamic payloads. *Int. J. Rob. Res.* **29**, 547–570 (2010).

67. S. B. Behbahani, X. Tan, Design and modeling of flexible passive rowing joint for robotic fish pectoral fins. *IEEE Trans. Robot.* **32**, 1119–1132 (2016).

68. Y. Zhao, M. Fukuhara, T. Usami, Y. Takada, Performance of very small robotic fish equipped with CMOS camera. *Robotics* **4**, 421–434 (2015).

69. A. Mazumdar, P. Valdivia y Alvarado, K. Youcef-Toumi, Maneuverability of a robotic tuna with compliant body, in *IEEE International Conference on Robotics and Automation 2008 (ICRA 2008)* (IEEE, 2008), pp. 683–688.

70. P. Valdivia y Alvarado, K. Youcef-Toumi, Design of machines with compliant bodies for biomimetic locomotion in liquid environments. *J. Dyn. Syst. Meas. Control.* **128**, 3–13 (2005).

71. S. L. Katz, D. A. Syme, R. E. Shadwick, High-speed swimming: Enhanced power in yellowfin tuna. *Nature* **410**, 770–771 (2001).

72. J. J. Videler, *Fish Swimming* (Springer Science & Business Media, 1993).

73. A. Maldonado-Ramírez, L. A. Torres-Méndez, F. Rodríguez-Telles, Ethologically inspired reactive exploration of coral reefs with collision avoidance: Bridging the gap between human and robot spatial understanding of unstructured environments, in *2015 IEEE/RSJ International Conference on Intelligent Robots and Systems (IROS)* (IEEE, 2015), pp. 4872–4879.

74. J. Halloy, G. Sempo, G. Caprari, C. Rivault, M. Asadpour, F. Tâche, I. Saïd, V. Durier, S. Canonge, J. M. Amé, C. Detrain, N. Correll, A. Martinoli, F. Mondada, R. Siegwart, J. L. Deneubourg, Social integration of robots into groups of cockroaches to control self-organized choices. *Science* **318**, 1155–1158 (2007).

75. Z. Butler, P. Corke, R. Peterson, D. Rus, From robots to animals: Virtual fences for controlling cattle. *Int. J. Rob. Res.* **25**, 485–508 (2006).

76. J.-H. Kim, S.-H. Choi, D. Kim, J. Kim, M. Cho, Animal-robot interaction for pet caring, in *2009 IEEE International Symposium on Computational Intelligence in Robotics and Automation (CIRA)* (IEEE, 2009), pp. 159–164.

77. T. Landgraf, R. Rojas, H. Nguyen, F. Kriegel, K. Stettin, Analysis of the waggle dance motion of honeybees for the design of a biomimetic honeybee robot. *PLOS ONE* **6**, e21354 (2011).

78. D. Romano, G. Benelli, C. Stefanini, Escape and surveillance asymmetries in locusts exposed to a Guinea fowl-mimicking robot predator. *Sci. Rep.* **7**, 12825 (2017).

79. N. Abaid, T. Bartolini, S. Macrì, M. Porfiri, Zebrafish responds differentially to a robotic fish of varying aspect ratio, tail beat frequency, noise, and color. *Behav. Brain Res.* **233**, 545–553 (2012).

80. F. Bonnet, Y. Kato, J. Halloy, F. Mondada, Infiltrating the zebrafish swarm: Design, implementation and experimental tests of a miniature robotic fish lure for fish-robot interaction studies, in *SWARM 2015: The First International Symposium on Swarm Behavior and Bio-Inspired Robotics* (2016), vol. 21, pp. 239–246.

81. P. Phamduy, G. Polverino, R. C. Fuller, M. Porfiri, Fish and robot dancing together: Bluefin killifish females respond differently to the courtship of a robot with varying color morphs. *Bioinspir. Biomim.* **9**, 036021 (2014).

82. S. Kalantar, U. R. Zimmer, Distributed shape control of homogeneous swarms of autonomous underwater vehicles. *Auton. Robots.* **22**, 37–53 (2007).

83. T. Schmickl, R. Thenius, C. Moslinger, J. Timmis, A. Tyrrell, M. Read, J. Hilder, J. Halloy, A. Campo, C. Stefanini, L. Manfredi, S. Orofino, S. Kernbach, T. Dipper, D. Sutantyo, CoCoRo—The self-aware underwater swarm, in *2011 Fifth IEEE Conference on Self-Adaptive and Self-Organizing Systems Workshops (SASOW)* (IEEE, 2011), pp. 120–126.

84. M. Read, C. Möslinger, T. Dipper, D. Kengyel, J. Hilder, R. Thenius, A. Tyrrell, J. Timmis, T. Schmickl, Profiling underwater swarm robotic shoaling performance using simulation, in *Towards Autonomous Robotic Systems* (Springer, 2013), *Lecture Notes in Computer Science*, pp. 404–416.

85. J. S. Jaffe, P. J. S. Franks, P. L. D. Roberts, D. Mirza, C. Schurgers, R. Kastner, A. Boch, A swarm of autonomous miniature underwater robot drifters for exploring submesoscale ocean dynamics. *Nat. Commun.* **8**, 14189 (2017).

86. N. Correll, Ç. D. Önal, H. Liang, E. Schoenfeld, D. Rus, Soft autonomous materials—Using active elasticity and embedded distributed computation, in *2012 Experimental Robotics: The 12th International Symposium on Experimental Robotics*, O. Khatib, V. Kumar, G. Sukhatme, Eds. (Springer, 2014), vol. 79 of *Springer Tracts in Advanced Robotics*, pp. 227–240.

87. C. D. Onal, D. Rus, Autonomous undulatory serpentine locomotion utilizing body dynamics of a fluidic soft robot. *Bioinspir. Biomim.* **8**, 026003 (2013).

88. G. V. Lauder, B. Flammang, S. Alben, Passive robotic models of propulsion by the bodies and caudal fins of fish. *Integr. Comp. Biol.* **52**, 576–587 (2012).

89. S. Alben, C. Witt, T. V. Baker, E. Anderson, G. V. Lauder, Dynamics of freely swimming flexible foils. *Phys. Fluids* **24**, 051901 (2012).

90. R. K. Katzschmann, A. de Maille, D. L. Dorhout, D. Rus, Cyclic hydraulic actuation for soft robotic devices, in *2016 IEEE/RSJ International Conference on Intelligent Robots and Systems (IROS)* (IEEE, 2016), pp. 3048–3055.

91. K. J. Åström, T. Hägglund, Revisiting the Ziegler–Nichols step response method for PID control. *J. Process Control* **14**, 635–650 (2004).

92. E. J. Tucholski, S. Traffic, *Underwater Acoustics and Sonar SP411 Handouts and Notes Fall 2006* (Physics Department, US Naval Academy, 2006).

93. D. H. Cato, Features of ambient noise in shallow water, in *Shallow Water Acoustics*, R. Zhang, J. Zhou, Eds. (China Ocean Press, 1997), pp. 385–390.

94. D. H. Cato, Marine biological choruses observed in tropical waters near Australia. *J. Acoust. Soc. Am.* **64**, 736–743 (1978).

95. L. Amundsen, M. Landrø, Marine seismic sources part VIII: Fish hear a great deal. *GEO ExPro* **8**, 42–46 (2011).

96. A. N. Popper, D. T. T. Plachta, D. A. Mann, D. Higgs, Response of clupeid fish to ultrasound: A review. *ICES J. Mar. Sci.* **61**, 1057–1061 (2004).

97. G. Goertzel, An algorithm for the evaluation of finite trigonometric series. *Am. Math. Mon.* **65**, 34–35 (1958).

Citation: R. K. Katzschmann, J. DelPreto, R. MacCurdy, D. Rus, Exploration of underwater life with an acoustically controlled soft robotic fish. *Sci. Robot.* **3**, eaar3449 (2018).

Science Robotics

Exploration of underwater life with an acoustically controlled soft robotic fish

Robert K. Katzschmann, Joseph DelPreto, Robert MacCurdy, and Daniela Rus

View the article online
https://www.science.org/doi/10.1126/scirobotics.aar3449
Permissions
https://www.science.org/help/reprints-and-permissions

Use of this article is subject to the Terms of service